



Prediction Model of Gas Expansion and Electro-Thermal Coupling regarding Lightning Damage to Carbon Fiber Composites

Yu Shi¹ · Bin Du¹ · Qian Liu¹ · Yuxiang Mai¹ · Yushun Zhao¹ · Jie Gao²

Received: 25 December 2020 / Accepted: 19 April 2021 / Published online: 21 May 2021
© The Author(s), under exclusive licence to Springer Nature B.V. 2021

Abstract

When carbon fiber reinforced polymer composites are struck by lightning, they are subjected to a combination of high-temperature ablation and gas expansion. To accurately predict the lightning damage area, the damage area of carbon fiber under different amounts of Joule heating was obtained through experiments, and a simulation analysis of electro-thermal coupling and gas expansion was performed. The simulation of electro-thermal coupling showed that the damage area of carbon fiber in the simulation accounts for 67% in the experiment at low energy, but there is a large gap between the two at high energy, with the former accounting for only 28.2% of the latter. Combining the effects of Joule heating and gas expansion and introducing the conversion efficiency of the Joule heat to the kinetic energy of gas, a damage prediction model of electrical-thermal–mechanical coupling was finally established. The calculation results of the composite model show that the maximum error between the model and the lightning test at high energy was only 12.5%. It was found that Joule heating has a greater impact on lightning damage at low energy, while gas expansion was the main factor in determining the damage degree of carbon fiber under the condition of high energy.

Keywords CFRP · Joule heating · Lightning experiment · Gas expansion · Damage prediction model

1 Introduction

Carbon fiber reinforced polymer (CFRP) composites are widely used in aerospace and military products because of their high mechanical strength, good corrosion resistance and light weight [1–4]. For example, the mass of the CFRP used in the structure of the Boeing 787 Dreamliner exceeds 50% of the total weight of the aircraft [5, 6]. However, the electrical conductivity

✉ Bin Du
dubin@hfut.edu.cn

¹ School of Electrical Engineering and Automation, Hefei University of Technology, Hefei 230009, People's Republic of China

² School of Life Sciences, Northwestern Polytechnical University, Xi'an 710129, People's Republic of China

and thermal conductivity of CFRP are relatively poor compared with those of metal materials. Aircraft are prone to spark discharge and material pyrolysis when struck by lightning, which seriously affect the flight safety of aircraft [7–9]. Therefore, research on the lightning damage mechanism and prediction model of composite materials has become a hot spot.

At present, a large number of experiments and simulations have been carried out on the lightning damage of CFRP. Harrell et al. used different lightning current waveforms to carry out experiments of lightning damage on CFRP. The results showed that the reduction in residual strength of CFRP was related to the amount of charge and specific energy and was more closely related to the specific energy [10]. The study showed that the current peak had a large influence on the damage area and the damage depth of CFRP, while the size and thickness of CFRP had almost no effect on the degree of damage [11]. Ogasawara et al. carried out a lightning experiment and an electro-thermal coupling simulation of CFRP and proposed two possible mechanisms of breakdown in the thickness direction of CFRP. One is the dielectric breakdown of the interlayer gas, which makes the current conduct along the thickness direction. The second is that Joule heating decomposes the surface carbon fiber and makes the material breakdown. At the same time, the material temperature in the simulation was consistent with the actual temperature when the latent heat was set, but there was still a gap between the simulation and the experimental results [12]. Dong added an analysis and a calculation of the resin pyrolysis degree on the basis of electro-thermal coupling and demonstrated the thermal damage behaviour involving the temperature, time and space by introducing a resin chemical reaction field [13]. Some scholars have conducted research on the influence of the thermal/electrical properties and the fiber direction of composite materials on lightning damage [14, 15]. The results showed that the electrical conductivity and specific heat had a power function relationship with the area of lightning ablation damage, but the thermal conductivity had no significant influence on the degree of ablation damage. In addition, the fiber direction of composite materials mainly affected the distribution of lightning current density, and the current density along the fiber direction was relatively high. Some studies assumed that constant pressure was applied within a certain radius to simulate the damage to CFRP by a pressure load [16, 17]. However, the damage area of the fiber was small in the simulation, and there was a gap relative to the experimental results, which indicated that the method of simulation with constant pressure had certain limitations. The influence of the BLOW-OFF impulse produced by the sublimation of carbon fiber on the damage of composite materials during a lightning strike is illustrated in Ref. [18]. It proved the importance of the BLOW-OFF impulse to the damage of composite materials. However, the influence of matrix sublimation was not considered in the simulation, indicating that the damage mechanism of gas shock waves on CFRP needs further study. CFRP is affected not only by the high voltage and electromagnetic force in the process of lightning strike but also by the high temperature and high-speed expansion of gas [12, 18]. Therefore, it is necessary to comprehensively consider the damage mechanism of Joule heating and gas expansion on CFRP, which is of great significance for accurately predicting the damage degree and remaining service life of CFRP.

Different amounts of Joule heating were used to carry out the experiments of lightning damage on CFRP in this study. The variation trend of the lightning discharge process and damage area of the carbon fiber under different amounts of Joule heating were also studied. Through the establishment of finite element simulation models, the effects of Joule heating and gas expansion on the lightning damage of CFRP were illustrated. An electrical-thermal-mechanical

multivariate prediction model of CFRP was established, and the calculation results showed that the model can predict the lightning damage degree of CFRP under different amounts of energy.

2 Experimental Program

2.1 Material

According to the ASTM D7137M-07 standard [19], the size of the CFRP sample is 150 mm×100 mm×2 mm. The type of carbon fiber is T300, the matrix material is epoxy resin, and the stacking sequence is $[45^\circ/0^\circ/-45^\circ/90^\circ]_2$. CFRP is made by the compression moulding method, in which a carbon fiber prepreg is made through processes such as coating and hot pressing and then prepared after high-temperature and high-pressure curing, as in Ref. [1, 20]. CFRP is an anisotropic structure, and there is a large difference in the mechanical properties in different directions. The coordinate system of the composite material is shown in Fig. 1. In the figure, 1, 2, and 3 are the fiber direction, perpendicular to the fiber direction and the thickness direction, respectively.

2.2 Experimental Device and Experimental Method

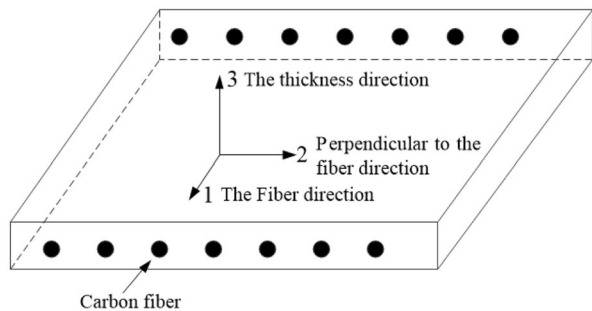
First, lightning damage experiments were carried out; the layout of the experimental platform is shown in Fig. 2. Both sides of the CFRP were fixed by copper clamps, and the four sides were evenly coated with conductive silver glue. The lightning current was introduced into the centre of the CFRP by a conical electrode, and the distance between the high-voltage electrode and the centre was 1 mm, as shown in Fig. 3. During the experiment, a camera (D5300, Nikon, Japan) was used to record the discharge process under different amounts of Joule heating, and a microscope (XP-3230, Tianzhu, China) was used to observe the microscopic morphology of the central area of the CFRP.

The current waveform of the lightning experiment was $8/20 \mu s$, and the peak values were 22 kA, 39 kA and 54 kA. Moreover, to facilitate further analysis, the Joule heat generated by the lightning current was 0.721 kJ, 2.231 kJ and 4.215 kJ according to Eq. (1).

$$Q_J = R_{eq} \int_0^t i^2(t) dt \tag{1}$$

where Q_J is the Joule heat, R_{eq} is the equivalent resistance of the CFRP, and $i(t)$ is the current value at different times.

Fig. 1 The CFRP coordinate system



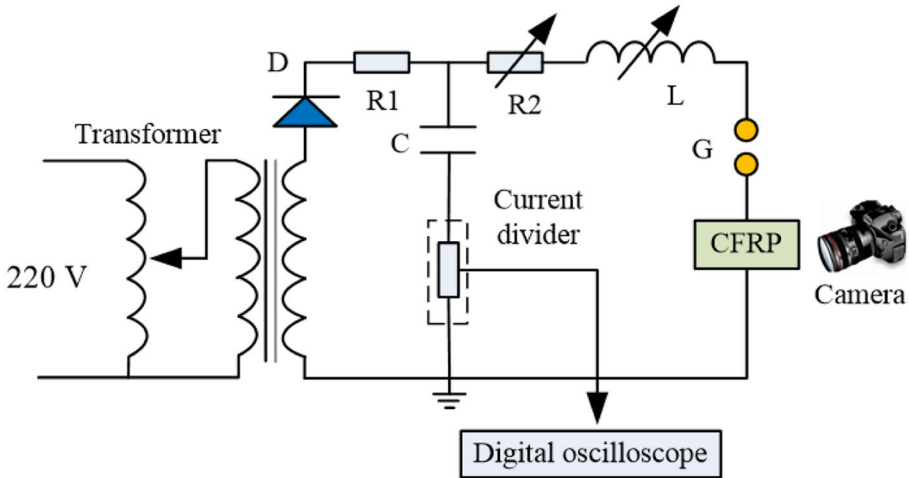


Fig. 2 Layout of the experimental platform

3 Experimental Results and Discussion

The discharge and lightning damage of CFRP at the initial time of lightning strike under different amounts of Joule heating are shown in Fig. 4. When the energy was 0.721 kJ, there was a bright discharge phenomenon in the area around the electrode. As the energy increased, the discharge became increasingly intense. When the energy reached 4.215 kJ, the electric spark generated by the discharge filled almost the entire space of the experimental device. When CFRP is struck by lightning, the carbon fiber at the centre is directly damaged by the lightning current, as shown in the red dashed box in Fig. 3. Under different amounts of Joule heating, the damage areas of the carbon fiber were 152 mm², 375 mm², and 585 mm². In addition, lightning strikes produce a large number of electric sparks that indirectly damage the carbon fiber. The gas pressure at the centre of the lightning strike also causes certain deformation of the material. The electric spark and gas pressure cause discontinuous linear damage on the CFRP surface, as shown by the yellow dashed box in Fig. 4.

Fig. 3 Fixture of the lightning experiment

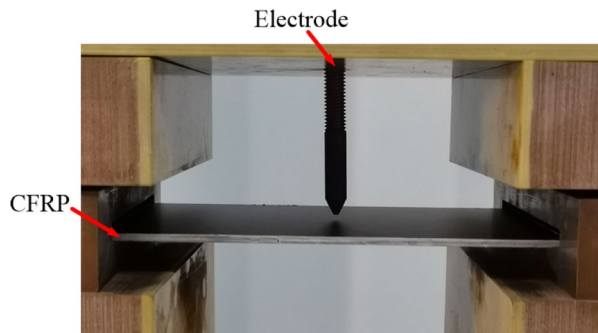
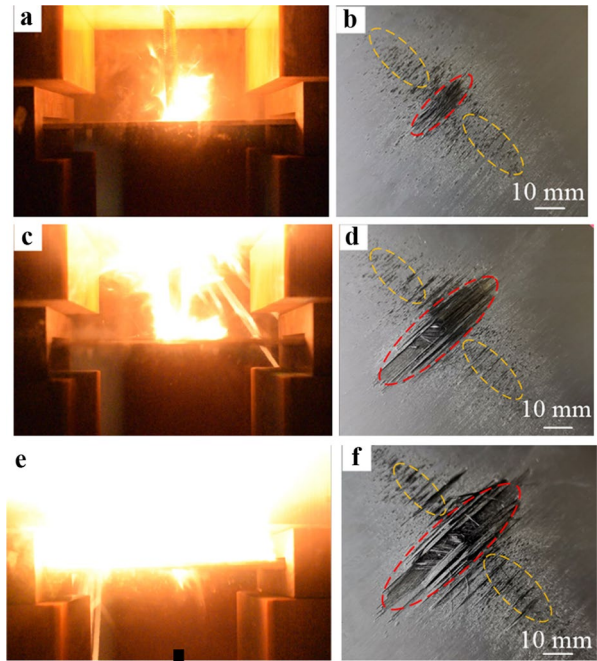


Fig. 4 Discharge and lightning damage of CFRP under different amounts of Joule heating (a), (b) 0.721 kJ; (c), (d) 2.231 kJ; (e), (f) 4.215 kJ



4 Numerical Analysis

4.1 Electro-Thermal Coupling Simulation

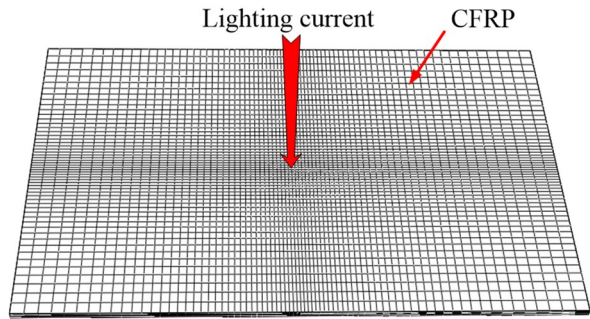
4.1.1 Simulation Model

The mathematical relationship of electro-thermal coupling can be expressed by the charge conservation equation and Fourier heat conduction equation [13]. The finite element software ABAQUS was used to simulate the damage to CFRP caused by Joule heating during a lightning strike; the 3D finite element model of CFRP is shown in Fig. 5. The lightning current peaks were 22 kA, 39 kA and 54 kA in the simulation. A lightning current with a waveform of $8/20 \mu\text{s}$ was applied to the centre of the CFRP. It was assumed that the potentials on the four sides of the CFRP were all 0 V. The thermal radiation coefficient was set to 0.9, and the initial temperature of the CFRP and the ambient temperature were both $25 \text{ }^\circ\text{C}$ [8]. The grid was divided by gradual encryption from both sides to the centre. The electrical characteristics of CFRP are shown in Table 1 [8, 21].

4.1.2 Simulation Results and Analysis

The temperature distribution on the surface of the CFRP at the end of- lightning strike is shown in Fig. 6. When the temperature reaches approximately $600 \text{ }^\circ\text{C}$, the carbon fiber is degummed [4], and the carbon fiber sublimates at approximately $3000 \text{ }^\circ\text{C}$ [9].

Fig. 5 Three-dimensional finite element model of CFRP for lightning strikes



Therefore, the area over 600 °C in the simulation was compared with the area where the carbon fiber was damaged in the experiment. The damaged area of the carbon fiber in the experiment and simulation is shown in Fig. 6. When the Joule heat was 0.721 kJ, 2.231 kJ, and 4.215 kJ, the damaged area of the carbon fiber in the simulation was 102 mm², 142 mm², and 165 mm², respectively.

The simulation results showed that the damage area of the carbon fiber increased slowly with increasing energy, while it increased rapidly in the experiment. When the energy was 0.721 kJ and 4.215 kJ, the simulated damage area was 67% and 28.2% of the experimental measurement value, respectively. When the energy was low, the simulation and experiment had good consistency. However, the difference between the two damage areas became increasingly larger with increasing energy, which indicated that the impact of Joule heating on lightning damage was relatively small at high energy.

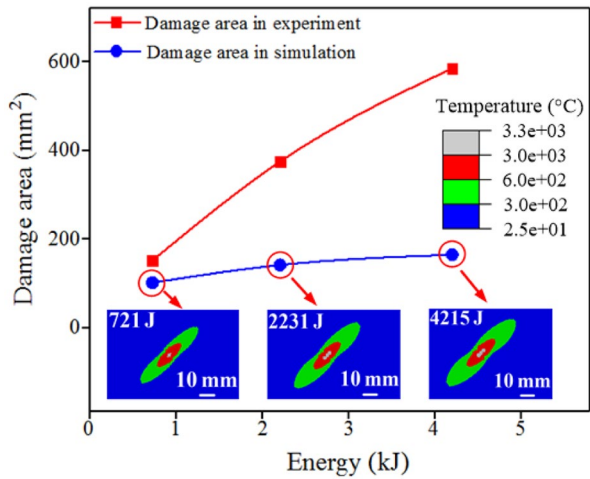
Lightning in nature can release a large amount of energy into a small air volume (approximately 10⁴–10⁵ J/m) within 10 μs; thus, the air is instantly heated to a high temperature, generating a very large amount of pressure [16]. At low energy, the energy transferred from Joule heat to gas is limited, and the amount of decomposition gas caused by high temperature is small. Therefore, the impact of gas expansion on the damage of carbon fiber is limited, and the high-temperature ablation caused by Joule heating is the main reason for the fracture of carbon fiber. With increasing energy, the energy transferred from Joule heat to gas also increases, and the volume of the pyrolysis gas increases. The gas produces a high pressure on the surface and inside the CFRP and forms a strong gas shock. The explosive shock forms in a short time and causes severe fracture and deformation of the carbon fiber. The damage diagram of the gas expansion relative to the CFRP is shown in Fig. 7.

Table 1 Electrical characteristics of CFRP

Temperature (°C)	Density (10 ⁶ kg m ⁻³)	Specific heat (J(kg °C) ⁻¹)	Electrical conductivity (Ω mm) ⁻¹		
			Longitudinal	Transverse	Through-thickness
25	1.52	1065	35.97	1.1 × 10 ⁻³	3.9 × 10 ⁻⁶
300	1.52	2100	35.97	1.1 × 10 ⁻³	3.9 × 10 ⁻⁶
600	1.10	2100	35.97	1.1 × 10 ⁻³	3.9 × 10 ⁻⁶
3316	1.10	2509	35.97	1.1 × 10 ⁻³	0.1
3334*	1.10	5875	35.97	2	1 × 10 ⁶

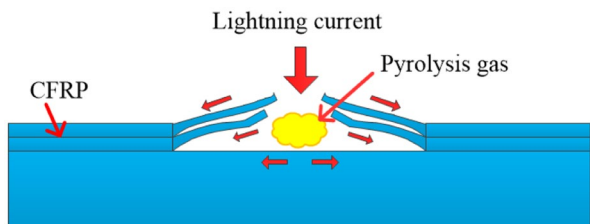
*- At this temperature, CFRP is in the gas state

Fig. 6 Surface temperature distribution and damage area versus energy curve of CFRP



When CFRP is struck by lightning, the composite material is thermally decomposed, producing a large amount of pyrolysis gas. The high temperature causes the pyrolysis gas to expand violently, which further intensifies the damage to the CFRP. A macroscopic enlarged view of the lightning damage to carbon fiber is shown in Fig. 8a. Through visual observation, the carbon fiber was obviously everted after being struck by lightning, and the carbon fiber bundles at the centre were very irregularly arranged and showed signs of severe ablation. In addition, the micro-morphology of carbon fiber in the central area of the lightning strike was magnified 100 times by a microscope, as shown in Fig. 8b. The carbon fiber bundle at the centre of the lightning strike was severely deformed and fractured and dispersed into multiple stray fiber filaments exposed on the surface of the CFRP. Due to the large impact force generated by gas expansion, the fiber filaments were subjected to mechanical force to break and diverge outward. If CFRP is subjected only to Joule heating, the fiber will not be warped and deformed in a wide range. The results showed that CFRP was not only ablated by Joule heating but also subjected to strong gas impact.

Fig. 7 Damage diagram of pyrolysis gas to CFRP



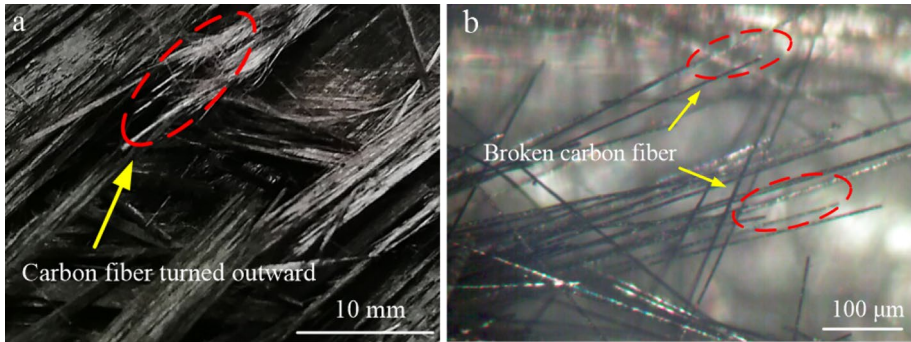


Fig. 8 Morphology of broken carbon fiber bundle: a macro-morphology; b micro-morphology

4.2 Gas Expansion Simulation

4.2.1 Mathematical Analysis

To simulate the damage process of gas shock waves relative to carbon fiber, a physical model of the damage generated by gas expansion onto CFRP was established. The pressure generated by gas expansion can be expressed by Eq. (2), where the expanded gas was equivalent to a spherical load, and the parameters of the expansion load are given in Ref. [22]. The pressure generated by a gas shock wave is:

$$P = A \left(1 - \frac{\omega}{R_1 V} \right) e^{-R_1 V} + B \left(1 - \frac{\omega}{R_2 V} \right) e^{-R_2 V} + \frac{\omega}{V} E_0 \tag{2}$$

where P is the pressure, V is the relative volume (the ratio of the volume of the gas expansion product to the initial volume), E_0 is the initial specific internal energy of the material, and $A, B, R_1, R_2,$ and ω are the material function coefficients.

The three-dimensional Hashin criterion was used to judge the mechanical damage to carbon fiber caused by gas expansion [23]. The damage to carbon fiber includes tensile damage and compression damage, which can be expressed by Eqs. (3) and (4), respectively.

Fiber tensile damage ($\sigma_{11} \geq 0$)

$$\frac{\sigma_{11}^2}{X_T^2} + \left(\frac{\sigma_{12}}{S_{12}} \right)^2 + \left(\frac{\sigma_{13}}{S_{13}} \right)^2 = \begin{cases} \geq 1 & \text{failure} \\ < 1 & \text{no failure} \end{cases} \tag{3}$$

Fiber compression damage ($\sigma_{11} < 0$)

$$\frac{\sigma_{11}^2}{X_c^2} = \begin{cases} \geq 1 & \text{failure} \\ < 1 & \text{no failure} \end{cases} \tag{4}$$

where X_T is the tensile strength in the fiber direction, X_c is the compressive strength in the fiber direction, S_{ij} is the shear strength in all directions of CFRP, and σ_{ij} is the stress in each direction of CFRP.

To truly reflect the process of instantaneous deformation, logarithmic strain is used to represent the deformation of CFRP by mechanical extrusion. If the instantaneous

length of a sample is l during uniaxial stretching and the length of the sample extends dl at the next moment, then the strain increment is:

$$d\varepsilon = \frac{dl}{l} \tag{5}$$

The sample is stretched from the initial length l_0 to the length l_1 , and the total strain is obtained by integrating along the stretching direction:

$$\varepsilon = \int_{l_0}^{l_1} \frac{dl}{l} = \ln \frac{l_1}{l_0} \tag{6}$$

where ε reflects the actual deformation of the object and is called the logarithmic strain.

4.2.2 Simulation Model

To simulate the mechanical damage to CFRP caused by gas expansion during lightning strike, the violent expansion of air was considered equivalent to the process of releasing energy from expanding gas, and the assembly of the CFRP and expansion load was established by the finite element software ABAQUS, as shown in Fig. 9. In the simulation, it was assumed that the side of the CFRP was fixed and that the material did not rotate during the damage process of gas expansion. The mechanical properties of CFRP are shown in Table 2 [24–26]. The expansion load was spherical and placed above the centre of the CFRP. In the simulation, the energy released by gas expansion was changed by changing the initial volume of the load.

In the simulation, the seriously distorted elements were deleted to prevent the serious distortion of elements from affecting the convergence of the simulation. The maximum principal strain and minimum principal strain were introduced into the element deletion criterion as follows [27]:

$$\varepsilon_{\max} - \varepsilon_M = \begin{cases} \geq 0 & \text{deleted} \\ < 0 & \text{not deleted} \end{cases} \tag{7}$$

$$\varepsilon_{\min} - \varepsilon_N = \begin{cases} \leq 0 & \text{deleted} \\ > 0 & \text{not deleted} \end{cases} \tag{8}$$

where ε_{\max} and ε_{\min} are the maximum and minimum principal strains of the material, respectively, and ε_M and ε_N are the maximum strain threshold and minimum strain threshold, which are set to 1 and -0.5, respectively.

Fig. 9 Three-dimensional finite element model of CFRP and expansion load

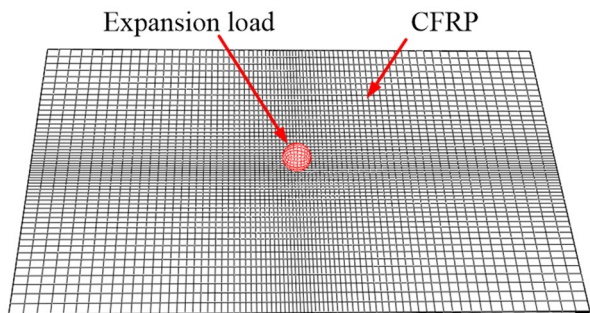


Table 2 The mechanical properties of CFRP

Property	Value	Property	Value
E_{11} (MPa)	139,700	ν_{23}	0.4
E_{22} (MPa)	12,900	X_T (MPa)	1871
E_{33} (MPa)	12,900	X_C (MPa)	1297
G_{12} (MPa)	6960	Y_T (MPa)	59.7
G_{13} (MPa)	6960	Y_C (MPa)	215
G_{23} (MPa)	3240	S_{12} (MPa)	102
ν_{12}	0.23	S_{23} (MPa)	109
ν_{13}	0.23	S_{13} (MPa)	109

Here, E_{11} , E_{22} and E_{33} are elastic moduli, ν_{12} , ν_{13} and ν_{23} are Poisson's ratios, G_{12} , G_{13} and G_{23} are shear moduli, X_T is the tensile strength in the fiber direction, X_C is the compressive strength in the fiber direction, Y_T is the tensile strength in the direction perpendicular to the fiber, Y_C is the compressive strength in the direction perpendicular to the fiber, and S_{12} , S_{23} , and S_{13} are the shear strength

4.2.3 Simulation Results and Analysis

The logarithmic strain of CFRP surfaces under expansion loads of different amounts of energy is shown in Fig. 10. With increasing energy, the area of the surface deformation of CFRP also increases. The deformation degree of the central region was the most serious, and it expanded along the longitudinal and transverse directions of the fiber. The logarithmic strain of the most severely distorted area can reach more than 0.6. Since the transverse elastic moduli of CFRP was smaller than the longitudinal elastic moduli, CFRP was more

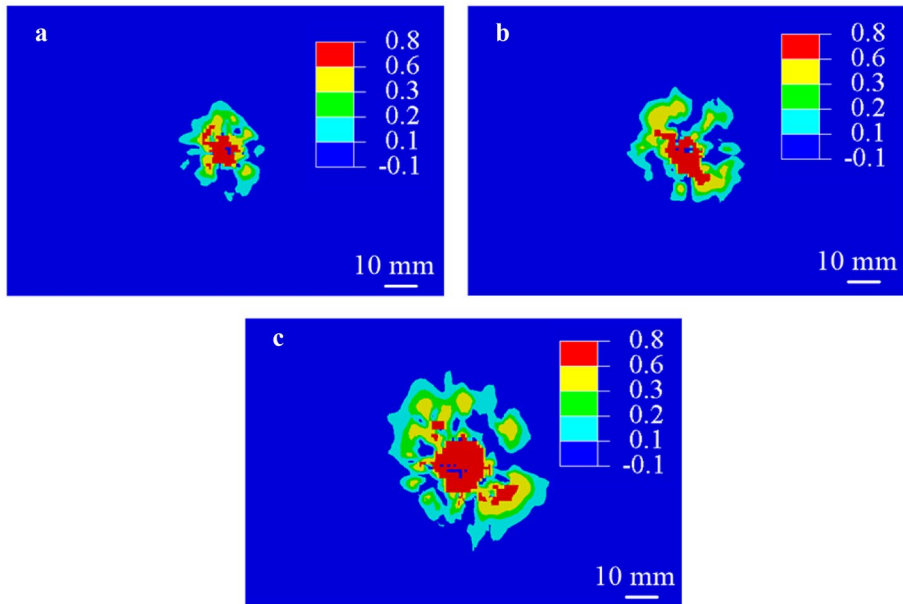


Fig. 10 Logarithmic strain of CFRP under expansion loads of different amounts of energy **a** 0.668 kJ; **b** 2.173 kJ; **c** 4.245 kJ

likely to deform in the transverse direction, and the transverse deformation range was larger than that in the longitudinal direction. The brittleness of carbon fiber is greater than that of epoxy resin. When a gas shock wave makes a carbon fiber reach its ultimate strength, the carbon fiber easily breaks without significant plastic deformation. In the experiment, CFRP produced an obvious fiber fracture along the longitudinal direction, and the direction perpendicular to the fiber had significant compression marks, which was consistent with the simulation results.

The morphology of the tensile damage and compression damage of carbon fiber on the surface of CFRP under different amounts of energy is shown in Fig. 11, where the red dots represent the damage area of the carbon fiber. The compression damage area, tensile damage area and total damage area of the carbon fiber in the simulation are shown in Table 3, and the curve of the damage area is shown in Fig. 12. The simulation showed that the tensile damage area was larger than the compression damage area under the same energy. The former was mainly concentrated in the central area of the expansion load, and the latter was concentrated outside the central area and distributed along the longitudinal direction of the fiber. The growth rate of the damage area of the fiber caused by gas expansion at low energy was faster, but the growth rate of the damage area slowed down at high energy.

4.3 A Model for Estimating the Damage Area

When considering only Joule heating, the relationship between the energy and the damage area of carbon fiber in the simulation agrees with Eq. (9), and the fitting degree R^2 is 0.9956.

$$S_1 = MQ_J^N = M \left[R_{\text{eq}} \int_0^t i^2(t) dt \right]^N \tag{9}$$

where S_1 is the damage area of carbon fiber caused by Joule heating (unit: mm^2), $M = 112$, and $N = 0.27$.

When considering only gas expansion, the relationship between the kinetic energy of gas and the damage area of carbon fiber conforms to Eq. (10), and the fitting degree R^2 is 0.9966.

$$S_2 = JQ_s^H = J \left[\beta R_{\text{eq}} \int_0^t i^2(t) dt \right]^H \tag{10}$$

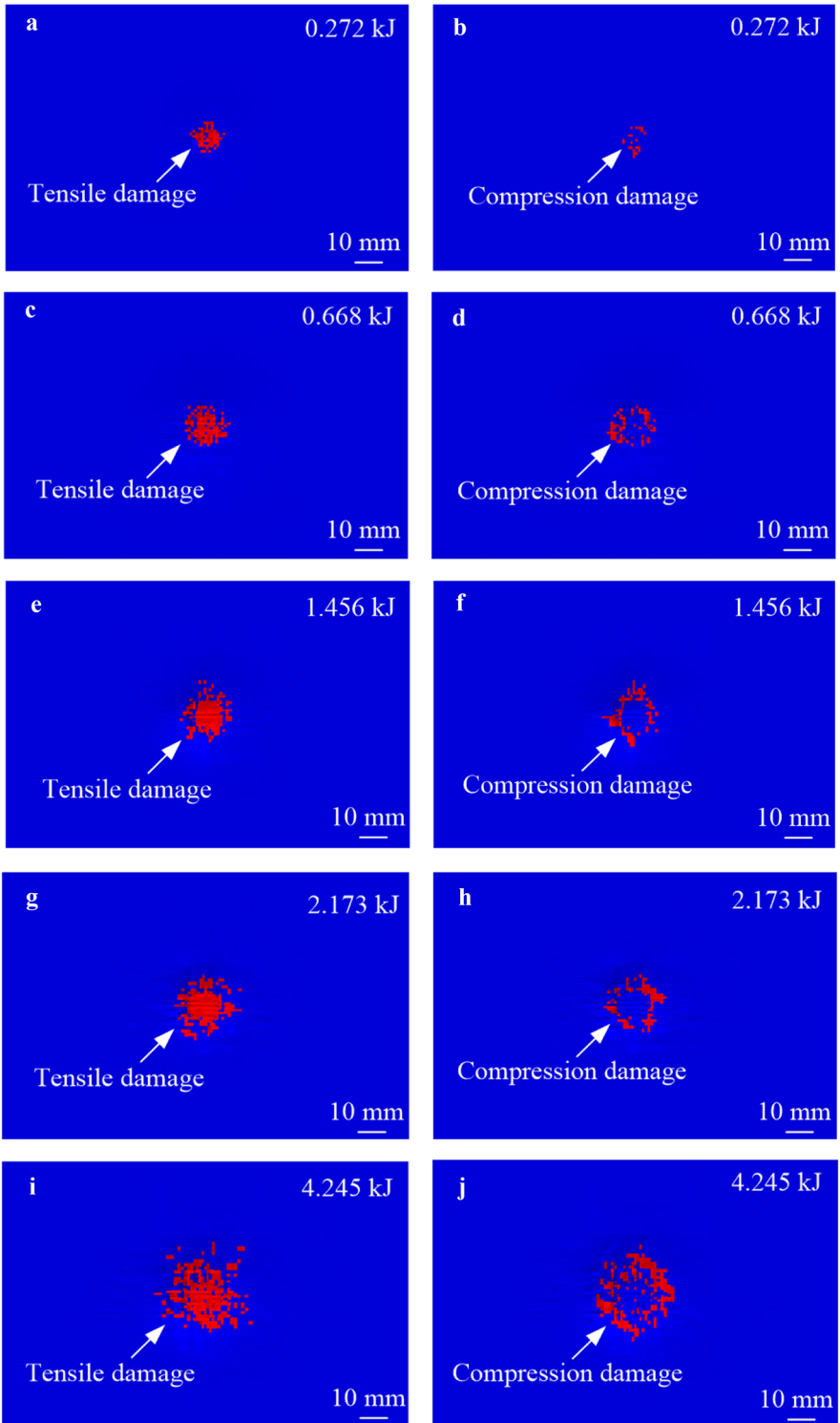
where S_2 is the damage area of carbon fiber in the gas expansion simulation (unit: mm^2), Q_s is the energy of the expanding gas (unit: kJ), β is the conversion efficiency of Joule heat to the kinetic energy of gas, $J = 205$, and $H = 0.71$.

Combining Eq. (9) and Eq. (10), the total damage area of the carbon fiber in CFRP caused by lightning is:

$$S = S_1 + S_2 = M \left[R_{\text{eq}} \int_0^t i^2(t) dt \right]^N + J \left[\beta R_{\text{eq}} \int_0^t i^2(t) dt \right]^H \tag{11}$$

where S is the total damage area of the carbon fiber (unit: mm^2).

Part of the Joule heat generated during a lightning strike is converted into kinetic energy of the gas, and the remaining energy is mainly volatilized in the form of heat energy. The efficiency of gas combustion and expansion is approximately 60% [28]. Based on this, we



◀**Fig. 11** Morphology of fiber damage under different amounts of energy. Fiber tensile damage: **a** 0.272 kJ; **c** 0.668 kJ; **e** 1.456 kJ; **g** 2.173 kJ; **i** 4.245 kJ. Fiber compression damage: **b** 0.272 kJ; **d** 0.668 kJ; **f** 1.456 kJ; **h** 2.173 kJ; **j** 4.245 kJ

Table 3 Comparison of fiber damage simulations under different amounts of energy

Energy (kJ)	Tensile damage area of fiber in simulation (mm ²)	Compression damage area of fiber in simulation (mm ²)	Damage area of fiber in simulation (mm ²)
0.272	56	21	77
0.668	99	69	168
1.456	150	102	252
2.173	239	123	362
4.245	347	231	578

set three conversion efficiencies of 50%, 60% and 70% to simulate the damage caused by gas expansion. Considering the effects of Joule heating and gas expansion comprehensively, the calculated values of the composite model under different efficiencies are shown in Table 4. The relationship curve between the damage area of carbon fiber and the amount of Joule heating is shown in Fig. 13.

When combined with the influencing factors of Joule heating and gas expansion, the carbon fiber damage area calculated by the electric-thermal-mechanical composite model is in good agreement with the experimental results, and the calculation error of the composite model at high energy is smaller than that at low energy. Under the condition of high energy, the damage to carbon fiber is relatively less affected by Joule heating. However, the high temperature causes the air to expand rapidly in a short time, and the gas shock wave under high temperature and high pressure causes the carbon fiber in the material to fracture over a wide range.

Fig. 12 Curve of the damage area in the gas expansion simulation

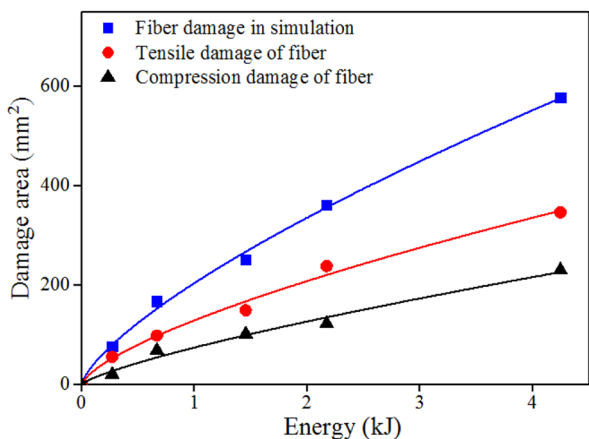
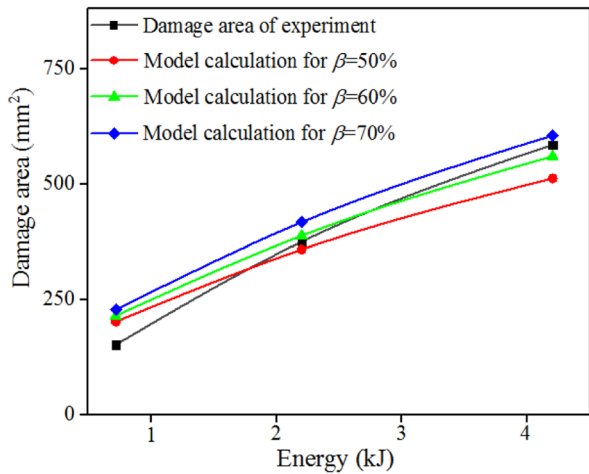


Table 4 Comparison of the damage area between the calculated value of the composite model and the experimental value

Energy (kJ)	Value of model calculation (mm ²) ($\beta = 50\%/60\%/70\%$)	Damage area of experiment (mm ²)	Error (%) ($\beta = 50\%/60\%/70\%$)
0.721	202/215/228	152	32.9/41.4/50.0
2.231	358/388/417	375	4.5/3.5/11.2
4.215	512/560/605	585	12.5/4.3/3.4

where β is the conversion efficiency of Joule heat to the kinetic energy of gas.

Fig. 13 Comparison of the experimental area and calculated area of the composite model

5 Conclusions

Through experiments and simulations, a new damage prediction model was established. The model fully considers the influence of gas expansion on the lightning damage to carbon fiber and compares the lightning damage area under different conversion efficiencies. It was assumed that the electric-thermal coupling and gas expansion were independent of each other, and the calculation results of the composite model showed that the assumption was basically consistent with the experimental results. The main conclusions and prospects are as follows:

- 1) Through the comparison between the electro-thermal coupling simulation and the experiments of lightning damage on CFRP when the Joule heat was 0.721 kJ and 4.215 kJ, the simulated damage area accounted for 67% and 28.2% of the experimental damage area, respectively. The results showed that the lightning damage to carbon fiber was greatly affected by Joule heating at low energy but was relatively less affected at high energy. Through a visual observation and microscopic observation, the carbon fiber was found to be severely everted, fractured and deformed, which indicated that carbon fiber is not only ablated by Joule heating but also affected by the strong gas impact.
- 2) We established a gas expansion model to simulate the damage process of carbon fiber caused by gas expansion. The simulation results showed that material deformation at

the centre of a lightning strike is the most serious, and the centre logarithmic strain can reach more than 0.6. When the energy of gas expansion increases from 0.272 kJ to 4.245 kJ, the area of fiber tensile damage increases from 56 mm² to 347 mm², and the area of fiber compression damage increases from 21 mm² to 231 mm². The fiber tensile damage area is larger than the fiber compression damage area under the same energy.

- 3) By introducing the conversion efficiency of the Joule heat to the kinetic energy of gas, we establish an electric-thermal–mechanical damage prediction model. When the Joule heat was 4.215 kJ, the maximum and minimum calculation errors of the composite model were 12.5% and 3.4%, respectively, which proved that the prediction model of Joule heating and gas expansion can predict lightning damage well.
- 4) The structure of actual aerospace materials is more complicated. For example, the outer layer of CFRP is usually covered with metal skin to give aircraft good aerodynamic performance, and metal fasteners are often used to establish mechanical connections with CFRP. The composite model established in this paper may yield a certain deviation in predicting the lightning damage to complex structures. The model will be improved for lightning damage to complex structures in future studies.

Acknowledgment This work was financially supported by the National Natural Science Foundation of China (grant no. 51707052)

Data Availability Statement The datasets generated during and analysed during the current study are available from the corresponding author on reasonable request.

References

1. Dong, Q., Wan, G.S., Guo, Y.L., Zhang, L.A., Wei, X.T., Yi, X.S., Jia, Y.X.: Damage analysis of carbon fiber composites exposed to combined lightning current components D and C. *Compos. A* **179**, 1–9 (2019)
2. Dong, Q., Wan, G.S., Xu, Y.Z., Guo, Y.L., Du, T.X., Yi, X.S., Jia, Y.X.: Lightning damage of carbon fiber/epoxy laminates with interlayers modified by nickel-coated multi-walled carbon nanotubes. *Appl. Compos. Mater.* **24**, 1339–1351 (2017)
3. Sun, J.R., Yao, X.L., Tian, X.Y., Chen, J.L., Yu, W.: Damage Characteristics of CFRP Laminates Subjected to Multiple Lightning Current Strike. *Appl. Compos. Mater.* **26**, 745–762 (2019)
4. Guo, Y.L., Xu, Y.Z., Wang, Q.L., Dong, Q., Yi, X.S., Jia, Y.X.: Enhanced lightning strike protection of carbon fiber composites using expanded foils with anisotropic electrical conductivity. *Compos. A* **117**, 211–218 (2018)
5. Kumar, V., Sharma, S., Pathak, A., Singh, B., Dhakate, S., Yokozeki, T., Okada, T., Ogasawara, T.: Interleaved MWCNT buckypaper between CFRP laminates to improve through-thickness electrical conductivity and reducing lightning strike damage. *Compos. Struct.* **210**, 581–589 (2019)
6. Feraboli, P., Miller, M.: Damage resistance and tolerance of carbon/epoxy composite coupons subjected to simulated lightning strike. *Compos. A* **40**, 954–967 (2009)
7. Fu, K.K., Ye, L., Chang, L., Yang, C.H., Zhang, Z.: Modelling of lightning strike damage to CFRP composites with an advanced protection system. Part I: Thermal–electrical transition. *Compos. Struct.* **165**, 83–90 (2017)
8. Yin, J.J., Li, S.L., Yao, X.L., Chang, F., Li, L.K., Zhang, X.H.: Lightning strike ablation damage characteristic analysis for carbon fiber/epoxy composite laminate with fastener. *Appl. Compos. Mater.* **23**, 821–837 (2016)
9. Abdelal, G., Murphy, A.: Nonlinear numerical modelling of lightning strike effect on composite panels with temperature dependent material properties. *Compos. Struct.* **109**, 268–278 (2014)

10. Harrell, T.M., Thomsen, O.T., Dulieu-Barton, J.M., Madsen, S.F.: Damage in CFRP composites subjected to simulated lightning strikes assessment of thermal and mechanical responses. *Compos. B* **176**, 1–11 (2019)
11. Hirano, Y., Katsumata, S., Iwahori, Y., Todoroki, A.: Artificial lightning experimenting on graphite/epoxy composite laminate. *Compos. A* **41**, 1461–1470 (2010)
12. Ogasawara, T., Hirano, Y., Yoshimura, A.: Coupled thermal- electrical analysis for carbon fiber/epoxy composites exposed to simulated lightning current. *Compos. A* **41**, 973–981 (2010)
13. Dong, Q., Guo, Y.L., Sun, X.C., Jia, Y.X.: Coupled electrical-thermal-pyrolytic analysis of carbon fiber/epoxy composites subjected to lightning strike. *Polymer* **56**, 385–394 (2015)
14. Yin, J.J., Chang, F., Li, S.L., Yao, X.L., Sun, J.R., Xiao, Y.: Lightning strike ablation damage influence factors analysis of carbon fiber/epoxy composite based on coupled electrical-thermal simulation. *Appl. Compos. Mater.* **24**, 1089–1106 (2017)
15. Audiffred, D., Possamai, T.S., Travassos, X.L., Ida, N.: Modeling electro-thermal effects of lightning strike on anisotropic composites. *Int. J. Appl. Electromagnet Mech* **62**, 557–575 (2020)
16. Modeling Lightning Impact Thermo-Mechanical Damage on Composite Materials: Muñoz R., Delgado S., González C., López-Romano B., Wang D., LLorca. J. *Applied Composite Materials* **21**, 149–164 (2014)
17. Foster, P., Abdelal, G., Murphy, A.: Quantifying the influence of lightning strike Pressure Loading on Composite Specimen Damage. *Appl. Compos. Mater.* **26**, 115–137 (2019)
18. Liu, Z.Q., Yue, Z.F., Wang, F.S., Ji, Y.Y.: Combining analysis of coupled electrical-thermal and BLOW-OFF impulse effects on composite laminate induced by lightning strike. *Appl. Compos. Mater.* **22**, 189–207 (2015)
19. Standard Test Method for Compressive Residual Strength Properties of Damaged Polymer Matrix Composite Plates. ASTM D7137M-07, American Society for Testing and Materials (ASTM), West Conshohocken, PA, USA. (2007)
20. Kamiyama, S., Hirano, Y., Okada, T., Ogasawara, T.: Lightning strike damage behavior of carbon fiber reinforced epoxy, bismaleimide, and polyetheretherketone composites. *Compos. Sci. Technol.* **161**, 107–114 (2018)
21. Foster, P., Abdelal, G., Murphy, A.: Understanding how arc attachment behaviour influences the prediction of composite specimen thermal loading during an artificial lightning strike test. *Compos. Struct.* **192**, 671–683 (2018)
22. Kong, D., Xu, Y., Song, C.: Dynamic repose of composites steel lining structure under blast Loading. *Shock. Vib.* **12**, 1–12 (2020)
23. Hashin, Z.: Failure criteria for unidirectional fiber composites. *J. Appl. Mech.* **47**, 329–334 (1980)
24. Reinoso, J., Catalanotti, G., Blázquez, A., Areias, P., Camanhod, P.P., París, F.: A consistent anisotropic damage model for laminated fiber-reinforced composites using the 3D-version of the Puck failure criterion. *Int. J. Solids Struct.* **126**, 37–53 (2017)
25. Rozylo, P., Debski, H., Wymulski, P., Falkowicz, K.: Numerical and experimental failure analysis of thin-walled composite columns with a top-hat cross section under axial compression. *Compos. Struct.* **204**, 207–216 (2018)
26. Li, X., Ma, D.Y., Liu, H.F., Tan, W., Gong, X.J., Zhang, C., Li, Y.: Assessment of failure criteria and damage evolution methods for composite laminates under low-velocity impact. *Compos. Struct.* **207**, 727–739 (2019)
27. Zhang, G.Q., Wang, B., Ma, L., Xiong, J., Wu, L.Z.: Response of sandwich structures with pyramidal truss cores under the compression and impact loading. *Compos. Struct.* **100**, 451–463 (2013)
28. Coney, M., Linnemann, C., Abdallah, H.: A thermodynamic analysis of a novel high efficiency reciprocating internal combustion engine-the isoengine. *Energy.* **29**, 2585–2600 (2004)